

Accelerated Bilateral DCE 3D Spiral Breast Imaging using TSENSE and Partial Fourier Methods

M. Han¹, B. L. Daniel², and B. A. Hargreaves²

¹Electrical Engineering, Stanford University, Stanford, CA, United States, ²Radiology, Stanford University, Stanford, CA, United States

Introduction: Dynamic contrast enhanced (DCE) breast MRI has shown great promise in discriminating benign and malignant breast lesions [1]. 3D spiral trajectories combined with a dual-band water-selective spectral-spatial excitation have been shown to suppress fat robustly while obtaining high spatio-temporal resolution in bilateral breast imaging [2]. Partial k-space acquisitions combined with undersampling in the slice encoding direction further increase temporal resolution for large 3D volume imaging of both breasts. Two well-known partial k-space reconstruction methods, homodyne and projection onto convex sets (POCS) have been incorporated with SENSE to reconstruct undersampled partial k-space data [3, 4]. In this work, we combined partial k-space reconstructions (both homodyne and POCS) with adaptive sensitivity encoding with temporal filtering (TSENSE) [5]. We show the results in simulated DCE phantom images and bilateral DCE breast images.

Methods: A 2D image with a 256 x 64 matrix simulating an axial bilateral breast image was made using a Shepp-Logan phantom with certain “tumor” areas enhancing over 48 temporal points (enhancement described by a general saturation equation [6]). “Normal tissue” enhancement, additive noise and slight motion were also incorporated and images were modulated by sensitivity maps calculated from actual multicoil water bottle images acquired with an 8 channel “VIBRANT” phased-array breast coil. For each temporal frame, alternately even and odd lines within 5/8 partial k-space were used. Patient bilateral breast images were acquired using a GE 1.5T Excite scanner, and the 8 channel breast coil. We used a 40° flip angle exciting a water-only slab over each breast, and a 3D stack of spirals imaging trajectory with 8 interleaves, TR of 27.9 ms, 20 x 20 cm FOV in-plane (resolution = 1.2 mm x 1.2 mm) and 32 phase-encoded k-space sagittal 3.4mm-thick planes per breast. With an acceleration factor of 2, we acquired phase encoded planes in a time-interleaved fashion, alternating between even and odd planes within 5/8 partial kz. The scan time per temporal frame (odd or even planes only) was 4.46s. Reconstruction was done in each axial reformatted plane after gridding in sagittal planes.

We applied the combination of TSENSE reconstruction with homodyne and POCS to simulated and patient data. Low-resolution full-FOV coil images were acquired by averaging the last 28 frames (post-contrast) from Hamming-windowed central symmetric k-space data. These coil images were normalized by square-root sum-of-squared magnitudes and used as sensitivity maps. For homodyne + TSENSE reconstruction, in each temporal frame, we used SENSE reconstruction for aliased images resulting both from central symmetric k-space and from asymmetric k-space pre-weighted by a ramp function. The complex image from asymmetric part was phase-corrected using the phase of low-resolution image from central k-space and the real part was taken as a final reconstructed image [3]. For POCS + SENSE reconstruction, the conventional POCS reconstruction was done on the undersampled k-space data with 3 iterations, then SENSE reconstruction was applied to the resulting image to get the full-FOV image [4]. For both reconstructions, slight residual artifacts were suppressed with temporal low pass filtering with a cut-off frequency of 0.425 relative to the sampling frequency (85 % bandwidth) for simulated data and 0.375 (75 % bandwidth) for breast data.

Results: Figure 1 shows simulated images from full k-space and reconstructed images using homodyne + TSENSE and POCS + TSENSE methods from undersampled partial k-space data. As illustrated in the 1D profiles plotted below the images, more spatial ringing artifacts result with homodyne + TSENSE in the regions where the signal phase changes rapidly (interface of two breasts) or magnitude changes rapidly. With POCS + TSENSE reconstruction, the signal enhancement curves match the original curves better than with homodyne + TSENSE. Figure 2 shows sagittal slices and reformatted axial slices reconstructed from homodyne + TSENSE and POCS + TSENSE from a patient. There were no visible aliasing artifacts from either method. Signal enhancement curves were measured in a ROI in an observable tumor and curves acquired from partial k-space reconstructions with and without undersampling are plotted for comparison. Using TSENSE, higher temporal resolution was achieved giving a steeper initial slope on the enhancement curve. The difference of signal magnitudes between homodyne + TSENSE and POCS + TSENSE may be explained by spatial ringing in the homodyne images.

Discussion: By combining partial Fourier reconstruction with TSENSE and 3D spiral imaging, temporal resolution of 7s was achieved in bilateral breast imaging. There were no observable aliasing artifacts from either homodyne + TSENSE or POCS + TSENSE. In images where there are rapid spatial variations in either magnitude or phase, as might occur in the case of a rapidly enhancing lesion, POCS + TSENSE might yield fewer phase artifacts than homodyne + TSENSE. The increased temporal resolution enabled by use of TSENSE plus partial k-space reconstruction should allow for better quantification of breast DCE data [7].

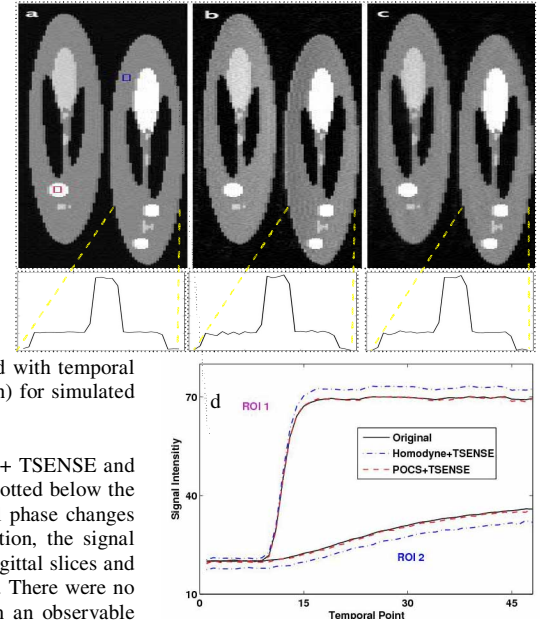


Figure 1: Simulated phantom data with signal enhancement. With the left-right phase encode direction, (a) full k-space image, (b-c) image reconstructed with homodyne + TSENSE (b) and POCS + TSENSE (c) from undersampled, partial k-space. 1D profiles crossing the simulated tumor were shown in the bottom (a-c). (d) Signal enhancement curves in ROIs shown in (a).

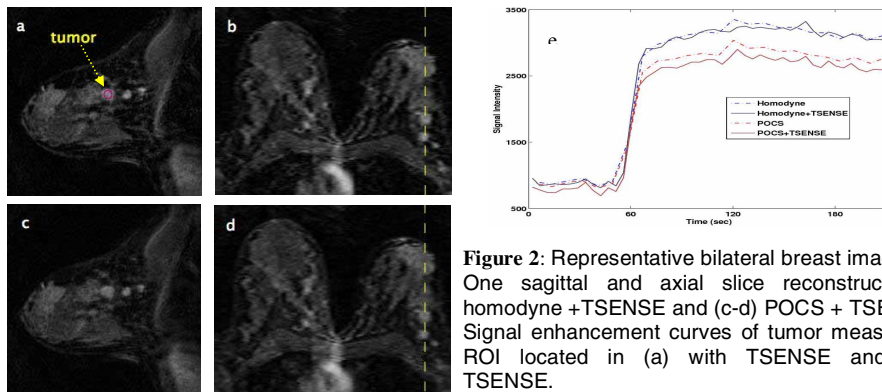


Figure 2: Representative bilateral breast images. (a-b) One sagittal and axial slice reconstructed from homodyne + TSENSE and (c-d) POCS + TSENSE. (e) Signal enhancement curves of tumor measured in a ROI located in (a) with TSENSE and without TSENSE.

References

1. Kuhl CK et al., Radiology, 211: 101-110, 1999.
2. Lee J et al., Proc., 14th ISMRM, p2871, 2006.
3. King KF et al., Proc., 8th ISMRM, p153, 2000.
4. Clayton DB et al., 13th ISMRM, p686, 2005.
5. Kellman P et al., MRM, 45: 846-852, 2001.
6. Morgan PH et al., Proc Natl Acad Sci, 72: 4327-4331, 1975.
7. Henderson E et al., MRM, 16 (9): 1057-73, 1998

Supported by NIH RR009784